



ELSEVIER

journal homepage: www.elsevier.com/locate/febsopenbio

Ornithine cyclodeaminase/ μ -crystallin homolog from the hyperthermophilic archaeon *Thermococcus litoralis* functions as a novel Δ^1 -pyrroline-2-carboxylate reductase involved in putative *trans*-3-hydroxy-L-proline metabolism

Seiya Watanabe^{a,*}, Yuzuru Tozawa^b, Yasuo Watanabe^a^a Faculty of Agriculture, Ehime University, 3-5-7 Tarumi, Matsuyama, Ehime 790-8566, Japan^b Proteo-Science Center, Ehime University, 3 Bunkyo-cho, Matsuyama, Ehime 790-8577, Japan

ARTICLE INFO

Article history:

Received 24 April 2014

Revised 25 June 2014

Accepted 7 July 2014

Keywords:

Ornithine cyclodeaminase

 Δ^1 -pyrroline-2-carboxylate reductase

Molecular evolution

trans-3-Hydroxy-L-proline metabolism

ABSTRACT

L-Ornithine cyclodeaminase (OCD) is involved in L-proline biosynthesis and catalyzes the unique deaminating cyclization of L-ornithine to L-proline via a Δ^1 -pyrroline-2-carboxylate (Pyr2C) intermediate. Although this pathway functions in only a few bacteria, many archaea possess OCD-like genes (proteins), among which only AF1665 protein (gene) from *Archaeoglobus fulgidus* has been characterized as an NAD⁺-dependent L-alanine dehydrogenase (AfAlaDH). However, the physiological role of OCD-like proteins from archaea has been unclear. Recently, we revealed that Pyr2C reductase, involved in *trans*-3-hydroxy-L-proline (T3LHyp) metabolism of bacteria, belongs to the OCD protein superfamily and catalyzes only the reduction of Pyr2C to L-proline (no OCD activity) [*FEBS Open Bio* (2014) 4, 240–250]. In this study, based on bioinformatics analysis, we assumed that the OCD-like gene from *Thermococcus litoralis* DSM 5473 is related to T3LHyp and/or proline metabolism (TILhpl). Interestingly, TILhpl showed three different enzymatic activities: AlaDH; N-methyl-L-alanine dehydrogenase; Pyr2C reductase. Kinetic analysis suggested strongly that Pyr2C is the preferred substrate. In spite of their similar activity, TILhpl had a poor phylogenetic relationship to the bacterial and mammalian reductases for Pyr2C and formed a close but distinct subfamily to AfAlaDH, indicating convergent evolution. Introduction of several specific amino acid residues for OCD and/or AfAlaDH by site-directed mutagenesis had marked effects on both AlaDH and Pyr2C reductase activities. The OCC_00387 gene, clustered with the TILhpl gene on the genome, encoded T3LHyp dehydratase, homologous to the bacterial and mammalian enzymes. To our knowledge, this is the first report of T3LHyp metabolism from archaea.

© 2014 The Authors. Published by Elsevier B.V. on behalf of the Federation of European Biochemical Societies. This is an open access article under the CC BY-NC-ND license (<http://creativecommons.org/licenses/by-nc-nd/3.0/>).

1. Introduction

L-Proline plays many important roles in the protein structure and cell signaling and is synthesized within cells and organisms from an intermediate, glutamate γ -semialdehyde, commonly involved in biosynthesis pathways from L-glutamate and L-arginine: L-glutamate \rightarrow γ -glutamyl phosphate \rightarrow glutamate γ -semialdehyde (Route 1); L-arginine \rightarrow L-ornithine \rightarrow glutamate γ -semialdehyde (Route 2) (Fig. 1A). The glutamate γ -semialdehyde then undergoes “non-enzymatic cyclization” to give the imine,

Δ^1 -pyrroline-5-carboxylate (Pyr5C), which is subsequently converted to L-proline by NAD(P)H-dependent Pyr5C reductase (EC 1.5.1.2) [1]. Route 1 is the main mechanism of L-proline biosynthesis in bacteria, while eukaryotes use this route predominantly under stress and limited nitrogen conditions. Under high nitrogen input, Route 2 appears to be prominent and is mainly found in higher plants.

Alternatively, L-proline is also directly synthesized from the amino acid L-ornithine, itself an intermediate along the above Route 2, by L-ornithine cyclodeaminase (OCD; EC 4.3.1.12) (Route 3) [2]. This unique enzyme initially catalyzes NAD⁺-dependent oxidative deamination from the α -amino group of L-ornithine, and subsequently cyclization to form Δ^1 -pyrroline-2-carboxylate (Pyr2C) (Fig. 1B). The actual cyclization step in this pathway occurs with the participation of enzymes, in contrast to glutamate γ -semialdehyde \rightarrow Pyr5C in Routes 1 and 2, described above. The final

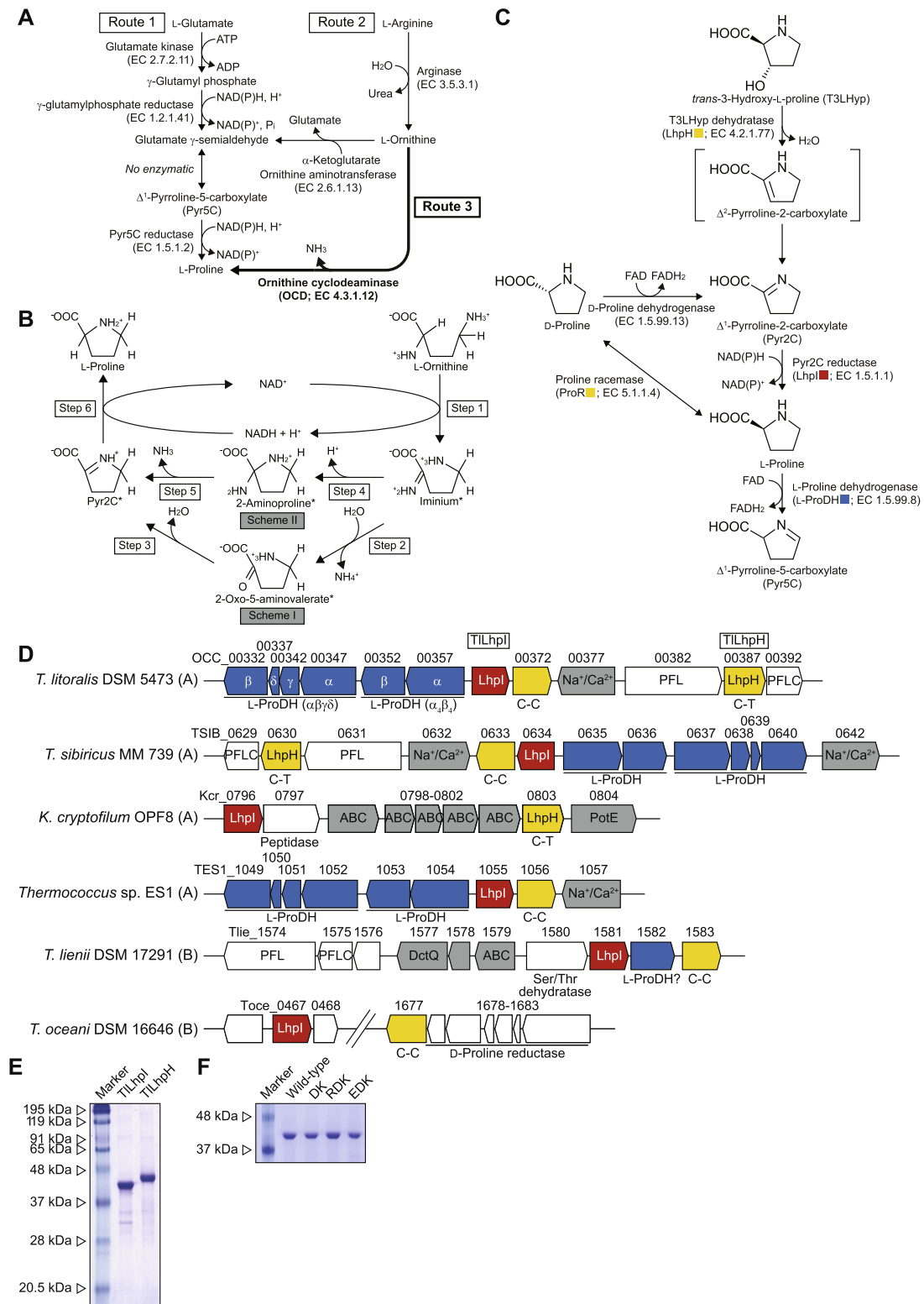
Abbreviations: OCD, ornithine cyclodeaminase; CRYM, μ -crystallin; AlaDH, L-alanine dehydrogenase; Pyr2C, Δ^1 -pyrroline-2-carboxylate; T3LHyp, *trans*-3-hydroxy-L-proline; NMAAlaDH, N-methyl-L-alanine dehydrogenase

* Corresponding author. Tel./fax: +81 89 946 9848.

E-mail address: irab@agr.ehime-u.ac.jp (S. Watanabe).

<http://dx.doi.org/10.1016/j.fob.2014.07.005>

2211-5463/© 2014 The Authors. Published by Elsevier B.V. on behalf of the Federation of European Biochemical Societies. This is an open access article under the CC BY-NC-ND license (<http://creativecommons.org/licenses/by-nc-nd/3.0/>).



step by OCD is NADH-dependent reduction of Pyr2C to L-proline. OCD belongs to the ornithine cyclodeaminase/ μ -crystallin (OCD/CRYM) superfamily (see Fig. 4). It was recently reported that μ -crystallin (CRYM) from mammals, known as an NADPH-dependent T3 thyroid hormone (triiodothyronin)-binding protein without enzymatic catalysis, functions as an NAD(P)H-dependent ketimine reductase (EC 1.5.1.25) [3]. Pyr2C is one of the substrates of this enzyme.

Although Route 3 of L-proline biosynthesis is found in several bacteria, including *Pseudomonas putida* [2], *Agrobacterium tumefaciens* [4], *Clostridium sporogenes* [5], and *Sinorhizobium meliloti* [6], many archaea possess OCD/CRYM family genes (proteins) (20–40% sequence identity with bacterial OCD). Among them, only AF1665 protein (gene) from the hyperthermophilic archaeon *Archaeoglobus fulgidus* has been characterized at the molecular level, and the protein functions as an L-alanine dehydrogenase (AlaDH; EC 1.4.1.1) but not OCD: L-alanine + NAD⁺ + H₂O \leftrightarrow pyruvate + NH₃ + NADH + H⁺ [7,8]. It is proposed that the enzyme (AfAlaDH) is involved in L-alanine metabolism (degradation), whereas the catalytic efficiency value for pyruvate is much higher than that for L-alanine. Although OCD activity is detected in a cell-free extract of *Methanococcus jannaschii* [9], no OCD/CRYM family gene is found on the genome. Up to now, the physiological role of OCD-like protein including AfAlaDH has been unclear in archaea.

There are two different mechanisms for OCD (Fig. 1B), in which L-ornithine is initially oxidized to an iminium (C _{α} = NH₂⁺ containing) intermediate (step 1 in Fig. 1B). In scheme I, the iminium undergoes hydrolysis to 2-oxo-5-aminovalerate by water before cyclization (step 2), and elimination of water produces Pyr2C (step 3). This scheme is analogous to the oxidative deamination of L-amino acid to 2-oxo acids by AlaDH [8], and has been preliminarily proposed based on biochemical experiments [10]. However, the crystal structure and molecular dynamic analysis of OCD [2,11] indicate an alternative mechanism (scheme II) that no attack on the iminium by water occurs: intramolecular cyclic addition of C-5 nitrogen of the iminium to the C-2 carbon to form 2-aminoproline (step 4), loss of ammonia, and reduction of the resulting imine, Pyr2C (step 5).

Recently, we characterized novel bacterial pathways of *trans*-4-hydroxy-L-proline (T4LHyp) and *trans*-3-hydroxy-L-proline (T3LHyp) metabolism [12,13]. In mammalian systems, T4LHyp and T3LHyp occur by post-translational hydroxylation of L-proline residue in certain proteins, in particular, collagen [14]. In contrast to T4LHyp, the metabolic pathways of T3LHyp from bacteria and mammals may be similar [13,15] and consist of two enzymes, T3LHyp dehydratase (encoded by *LhpH* gene; EC 4.2.1.77) and NAD(P)H-dependent Pyr2C reductase (encoded by *LhpI* gene; EC 1.5.1.1), by which T3LHyp is converted to L-proline via Pyr2C (Fig. 1C). Interestingly, *LhpI* protein is a novel member of the OCD/CRYM superfamily, and catalyzes only the reduction of Pyr2C to L-proline (no OCD activity) [11]. Furthermore, there is no sequence similarity to *DpkA* protein as is known for the reductase of Pyr2C from bacteria [16], strongly suggesting their convergent evolution.

Metabolism of T3LHyp (and T4LHyp) by archaea has been unclear until now, and it is impossible to further assess the physiological functions of OCD-like proteins in archaea based on a simple homology search. In this study, we selected OCD-like protein (gene) from a hyperthermophilic archaeon, *Thermococcus litoralis* DSM 5473, as a target, and this protein functions as an NAD(P)H-dependent Pyr2C reductase rather than AlaDH. This gene was clustered with T3LHyp dehydratase and proline racemase genes involved in putative T3LHyp and/or proline metabolism. Molecular evolution of the OCD/CRYM family is also discussed.

2. Results

2.1. Candidates of target genes

Although it is unclear whether there are archaea capable of metabolizing T3LHyp as a sole carbon source, a homology search by the Protein-BLAST program was carried out against genome sequences of archaea using bacterial Pyr2C reductases (*LhpI* from *Azospirillum brasilense* (AbLhpI), GenBank: BAO21622; *LhpI* from *Colwellia psychrerythraea* 34H (CpLhpI), GenBank: YP_268197) as the probe protein sequences. As described below, bacterial Pyr2C reductases are classified into two different subfamilies, in which CpLhpI and AbLhpI are contained, respectively (see Fig. 4). However, over 900 homologous genes (proteins) with sequence identities of 20–40% were found (data not shown). Similar results was also obtained when other OCD/CRYM family proteins including AfAlaDH was used instead of *LhpI* protein as the probe.

On the other hand, when bacterial T3LHyp dehydratases (*LhpH* from *A. brasilense* (AbLhpH), GenBank: BAO21621; *LhpH* from *C. psychrerythraea* 34H (CpLhpH), GenBank: YP_268195) was used as the probe, 31 homologous genes were found. T3LHyp dehydratase belongs to the proline racemase superfamily, which also includes the archetypical proline racemase (EC 5.1.1.4) and T4LHyp epimerase (EC 5.1.1.8) (Fig. S1) [15,17]. In contrast to bacterial Pyr2C reductases, T3LHyp dehydratase form a single subclass in this superfamily. On the basis of two specific residues at the active sites, the members have been classified into three types: Cys-Cys type (proline racemase and T4LHyp epimerase); Cys-Thr type (T3LHyp dehydratase); Ser-Cys type (function unknown). Furthermore, two Cys-Cys type enzymes can be clearly distinguished in the phylogenetic tree. Based on this insight, we could select only three proline racemase-like genes as putative T3LHyp dehydratases, although it has been believed that the enzyme is found only in animals and fungi (and bacteria) [13,15]: *T. litoralis* DSM 5473 (OCC_00387, GenBank: YP_008428263; 45.6% identity with AbLhpH), *Thermococcus sibiricus* MM 739 (TSIB_0630, GenBank: YP_002994044; 47.1%), and *Candidatus Korarchaeum cryptofilum* OPF8 (OPF8 Kcr_0803, GenBank: YP_001737233; 44.1%) (Fig. 1). Interestingly, these genes were clustered with OCD-like genes: *T. litoralis* (OCC_00362 \rightarrow YP_008428257 OCC_00367, GenBank: YP_008428258); *T. sibiricus* (TSIB_0634, GenBank: YP_002994048); *K. cryptofilum* (Kcr_0796, GenBank: YP_001737226) (Fig. 1D). In the cases of *T. litoralis* and *T. sibiricus*, another proline racemase-like gene (Cys-Cys type) and genes encoding two different types of putative heterooligomeric L-proline dehydrogenase (L-ProDH) [18,19] were also contained in this gene cluster. This analysis strongly indicated that the gene cluster is related to T3LHyp and/or proline metabolism. Therefore, in this study, we selected GenBank: OCC_00362, GenBank: OCC_00367, and GenBank: OCC_00387 genes from *T. litoralis* as target genes (referred to as *TILhpI* and *TILhpH* genes, respectively).

2.2. Preparation of recombinant His₆-tag proteins

TILhpI gene was fused with OCC_00362 and OCC_00367 genes by PCR (Supplementary Methods). After cloning all target genes into the vector pETDuet-1, the recombinant enzymes with attached His₆-tags at their N-termini were expressed in *Escherichia coli* and purified with an Ni²⁺-chelating affinity column (Fig. 1E). Apparent molecular masses of *TILhpI* and *TILhpH*, estimated by SDS-PAGE, were 40 (36.9) and 43 (38.1) kDa (values in parentheses indicate the calculated molecular mass of the enzyme with His₆-tag), and those estimated by analytic gel filtration were 72 and 75 kDa, respectively (data not shown). Therefore, the two enzymes appear to be dimeric.

2.3. Characterization of TILhpl as AlaDH

Although TILhpl shows only 44.3% sequence identity with AfAlaDH, we could detect both activities of the NAD^+ -dependent oxidative deamination of L-alanine and NADH -dependent reductive amination of pyruvate (in presence of 700 mM NH_4^+): specific activities of 0.0265 and 4.43 (unit/mg protein), respectively. NADP^+ was not used as a coenzyme. The optimum pH values of each reaction were 10–12 and 6–10.5, respectively (Fig. 2A). The k_{cat}/K_m value for pyruvate was ~ 230 -fold higher than that for L-alanine, caused by the ~ 120 -fold lower K_m value: namely, the reaction equilibrium favors the direction toward reductive amination (Tables 1 and 2). Activity was also observed with several L-amino acids and 2-oxo acids with a hydrophobic side chain (see below for L-proline). Among them, L-2-aminovalerate and 2-oxovalerate with a C_3

aliphatic side chain were the best substrates, and the k_{cat}/K_m values were 146- and 4.7-fold higher than those for L-alanine and pyruvate, respectively. When pyruvate and NADH were alternatively incubated together with methylamine (50 mM) instead of NH_4^+ as the nitrogen donor, reduction activity was detected. This result indicated that TILhpl functions not only as AlaDH but also N-methyl-L-alanine dehydrogenase (NMAlaDH; EC 1.4.1.17). Activities of AlaDH and NMAlaDH were also detected in HPLC analysis using the reaction products and zymogram staining analysis (Figs. 2B and 3A, B). k_{cat}/K_m values for L-alanine and pyruvate of TILhpl were over 1000-fold lower than those of AfAlaDH [7]. Furthermore, the K_m value for NH_4^+ of TILhpl was clearly beyond the physiological level (Table 2). AfAlaDH shows similar optimum pH of the oxidative and reductive reactions (~ 7.0), and no significant activity for hydrophobic amino acids including L-2-aminovalerate

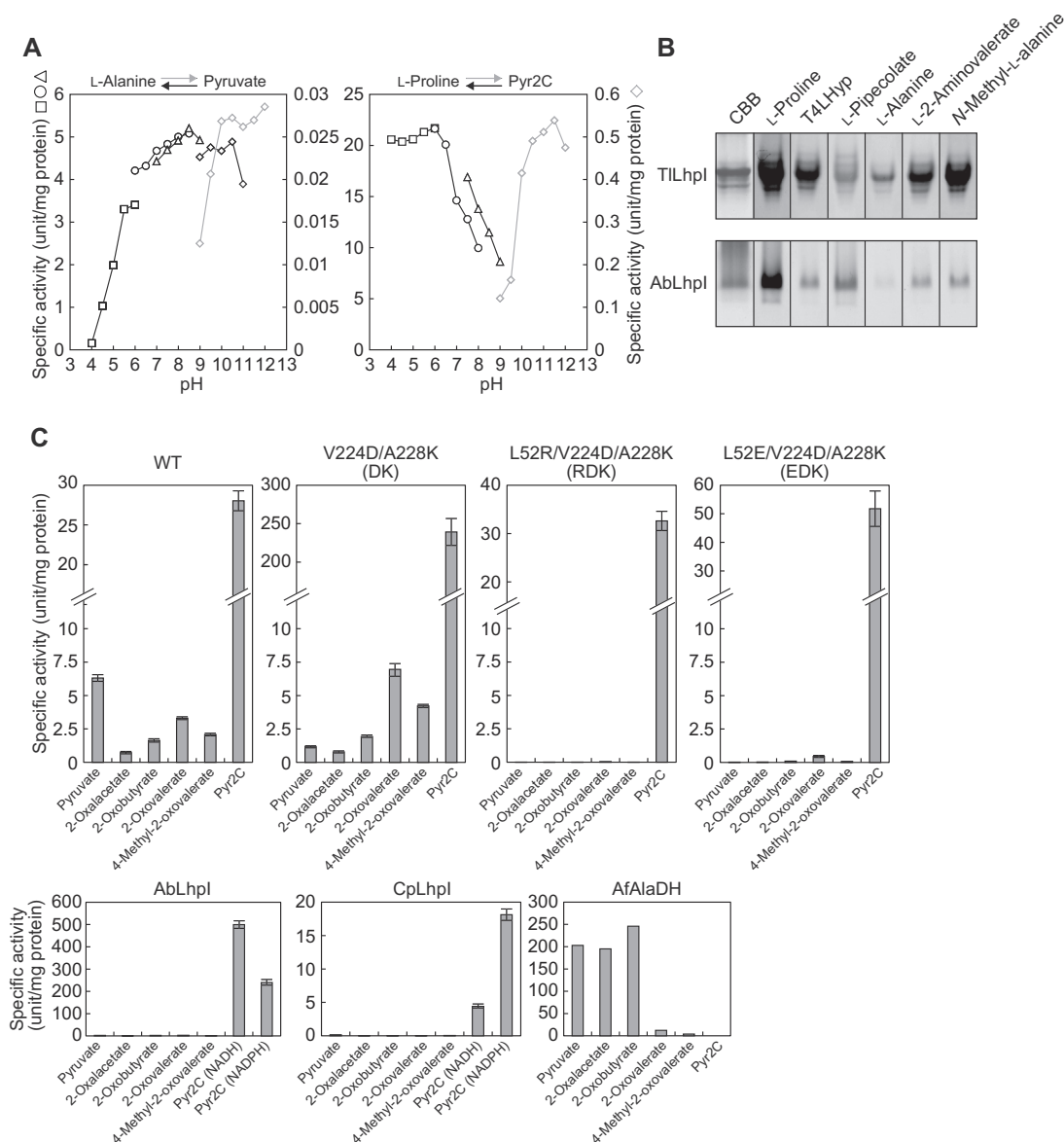


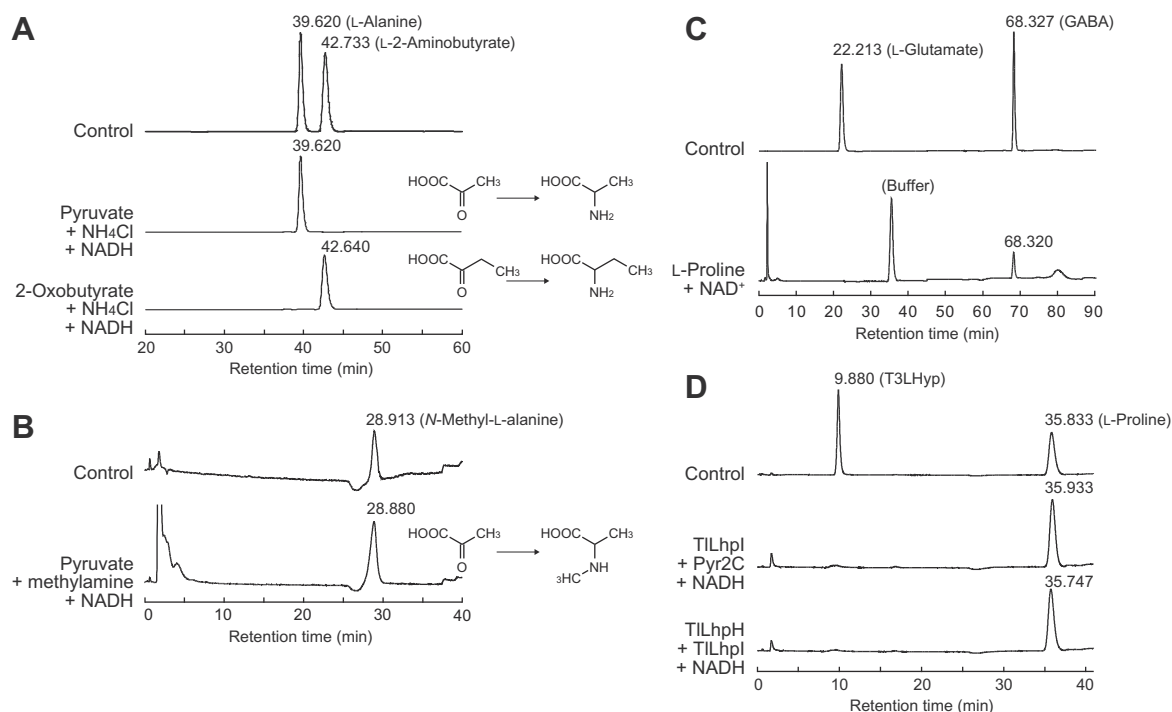
Fig. 2. Enzymatic properties of TILhpl Pyr2C. (A) Effect of pH on the activity as AlaDH (left panel) and Pyr2C reductase (right panel). 50 mM acetate-NaOH (pH 4.0–6.0) (square), 50 mM potassium phosphate (pH 6.0–8.5) (circle), 50 mM Tris-HCl (pH 7.0–9.0) (triangle) for the reduction of pyruvate or Pyr2C (left axis and black symbol), and 50 mM Bis-tris propane (diamond) for the oxidation of L-alanine or L-proline (right axis and gray symbol), instead of 50 mM buffer under each standard assay condition. (B) Zymogram staining. Five micrograms each of purified protein was applied on 10% (w/v) gel. After electrophoresis, the gel was soaked at 50 °C (for TILhpl) or 30 °C (for AbLhpl) in staining solution in the presence of the indicated substrate and NAD^+ (each of 10 mM). Protein stained with Coomassie Brilliant Blue (CBB) was used as a loading control. (C) Comparison of NADH -dependent AlaDH and Pyr2C reductase activities of wild-type and mutated TILhpl proteins. The assay was performed with standard assay solution containing the indicated substrate (10 mM). AbLhpl and CpLhpl were assayed at 30 °C under the standard assay conditions for TILhpl. Data for AfAlaDH are from Ref. [7].

Table 1
Kinetic parameters of NAD⁺-dependent oxidation reaction.

Enzymes	Substrates	Specific activity ^a (units/mg protein)	K _m (mM)	k _{cat} (min ⁻¹)	k _{cat} /K _m (min ⁻¹ mM ⁻¹)
Wild type	L-Alanine	0.0265 ± 0.0015	18.2 ± 5.0	2.64 ± 0.55	0.147 ± 0.012
	L-2-Aminobutyrate	0.136 ± 0.010	6.00 ± 0.29	6.71 ± 0.16	1.12 ± 0.03
	L-2-Aminovalerate	0.396 ± 0.030	0.306 ± 0.009	6.56 ± 0.08	21.5 ± 0.4
	L-Leucine	0.248 ± 0.010	1.32 ± 0.10	10.5 ± 0.4	8.00 ± 0.28
	N-Methyl-L-alanine	0.526 ± 0.025	0.406 ± 0.044	11.6 ± 0.7	28.6 ± 2.1
	L-Proline	0.384 ± 0.015 (0.0376 ± 0.0005) ^b	1.12 ± 0.12 (13.1 ± 1.2) ^b	13.8 ± 1.0 (3.27 ± 0.24) ^b	12.3 ± 0.4 (0.250 ± 0.006) ^b
V224D/A228K	L-Alanine	0.0133 ± 0.0010	36.9 ± 0.9	2.12 ± 0.02	0.0575 ± 0.0008
	L-2-Aminovalerate	0.666 ± 0.050	2.13 ± 0.30	7.72 ± 0.82	3.64 ± 0.12
	L-Proline	1.51 ± 0.10	0.444 ± 0.008	36.5 ± 0.9	82.2 ± 1.1

^a Under standard assay conditions in “Experimental procedures”. All substrate concentrations were 10 mM.^b NADP⁺-dependent activity.**Table 2**
Kinetic parameters of NADH-dependent reductive reaction.

Enzymes	Substrates	Specific activity ^a (units/mg protein)	K _m (mM)	k _{cat} (min ⁻¹)	k _{cat} /K _m (min ⁻¹ mM ⁻¹)
Wild type	Pyruvate	4.43 ± 0.50	9.37 ± 0.23	315 ± 4	33.6 ± 0.4
	Oxalacetate	1.78 ± 0.18	8.86 ± 0.91	192 ± 15	21.7 ± 0.5
	2-Oxobutyrate	2.46 ± 0.25	0.701 ± 0.020	92.0 ± 1.8	131 ± 1
	2-Oxovalerate	2.59 ± 0.21	0.969 ± 0.093	152 ± 11	157 ± 3
	4-Methyl-2-oxovalerate	1.02 ± 0.19	2.52 ± 0.45	129 ± 18	51.4 ± 2.0
	NH ₄ ⁺ (+2-oxovalerate) ^b	2.45 ± 0.22	1450 ± 240	267 ± 33	0.183 ± 0.007
	Pyr2C	23.9 ± 2.5	0.944 ± 0.090	995 ± 33	1058 ± 66
V224D/A228K	Pyruvate	1.60 ± 0.15	62.0 ± 12.2	413 ± 75	6.68 ± 0.11
	2-Oxovalerate	7.00 ± 0.95	1.82 ± 0.14	212 ± 16	116 ± 0
	Pyr2C	239 ± 35	2.77 ± 0.44	33500 ± 4900	12900 ± 300

^a Under standard assay conditions in “Experimental procedures”. All substrate concentrations were 10 mM.^b The NH₄⁺ concentrations were changed with a fixed concentration of 2-oxovalerate (10 mM).**Fig. 3.** HPLC analysis of the reaction products. (A) Reaction product from pyruvate or 2-oxobutyrate by TILhpl (as AlaDH) in presence of NADH and NH₄Cl. Control indicates authentic L-alanine and L-2-aminobutyrate. (B) Reaction product from pyruvate by TILhpl (as NMAIaDH) in the presence of NADH and methylamine. Control indicates authentic N-methyl-L-alanine. (C) Reaction product from L-proline by TILhpl (as L-ProDH) in the presence of NAD⁺. After the enzymatic reaction, the product was treated by H₂O₂, and then analyzed. Control indicates authentic L-glutamate and γ -aminobutyrate (GABA), which are potentially yielded from Pyr5C and Pyr2C, respectively. (D) Reaction products from Pyr2C by TILhpl and from T3LHyp by TILhpl and TILhpl, in the presence of NADH. Control indicates authentic T3LHyp and L-proline. No peak corresponding to Pyr2C was observed, probably caused by no reaction with labeling reagent for amino acid analysis (data not shown).

(2-oxoalate). This indicated strongly that TILhpl possesses largely different properties from AfAlaDH, and that the physiological function is not the metabolism of L-alanine and pyruvate.

2.4. Characterization of TILhpl as novel Pyr2C reductase in OCD/CRYM superfamily

In contrast to AfAlaDH [7], TILhpl showed NAD⁺-dependent oxidation activity for L-proline. The k_{cat}/K_m value in the presence of NAD⁺ was ~50-fold lower than that in the presence of NAD⁺ (Table 1): the specificity for NAD⁺ is described above. In addition to L-proline, several L-proline analogs, including *cis*-4-hydroxy-L-proline (85%), *trans*-4-hydroxy-L-proline (70%), and L-pipecolate (49%), were active substrates (relative activity to L-proline in parentheses), whereas it is known that bacterial Lhpl proteins are strictly specific to L-proline [13]. These activities were also detected in zymogram staining analysis (Fig. 2B). When the reaction product of L-proline was further oxidized by H₂O₂, 4-aminobutyrate (GABA) was identified in HPLC analysis (Fig. 3C), indicating that TILhpl catalyzes the conversion of L-proline to Pyr2C. Generally, L-ProDH (EC 1.5.99.8) including archaeal enzymes [18,19] is a flavoprotein, and the reaction product is Pyr5C (if so, L-glutamate is yielded by the above H₂O₂ treatment).

Therefore, we compared the dehydrogenation activity toward L-proline and other L-amino acids (Tables 1 and 2). The k_{cat}/K_m value for Pyr2C (1058 min⁻¹ mM⁻¹) was 6.7-fold higher than that for 2-oxoalate, caused by the high k_{cat} value. Furthermore, the ratio of Pyr2C to L-proline in k_{cat}/K_m was 86, suggesting the preference of the reaction equilibrium in the direction toward NADH-dependent reduction. Interestingly, the optimum pH of Pyr2C reductase was 4.0–6.0, clearly different from that of the reductive deamination of AlaDH (pH 6–10.5) (Fig. 2A). These results strongly indicated that Pyr2C is the preferred substrate for TILhpl. Although Ablhpl and CpLhpl showed only 25.3% and 31.6% sequence identity to TILhpl, respectively, we unexpectedly detected AlaDH activity in both enzymes (Fig. 3C). Commonly, these bacterial enzymes showed significantly high ratios of Pyr2C to pyruvate in specific activity: 176 and 28, respectively (~5 for TILhpl). Namely, TILhpl possessed “vestigial” properties to AlaDH, probably due to the close phylogenetic relationship between them, as described in the main section.

Using the reductase activity toward Pyr2C, several properties of TILhpl as an enzyme from “hyperthermophiles” were identified: *T. litoralis* grows between 55 and 98 °C with an optimal growth temperature of 88 °C [20]. Although the optimum temperature was above 75 °C, and clearly higher than that of (mesophilic) Ablhpl, the assay could not be performed above 75 °C due to the thermolability of NADH (Fig. S2A). Thus, TILhpl appears to be a typical (hyper)thermophilic enzyme.

2.5. Phylogenetic analysis of TILhpl

As expected from the preliminary annotation, TILhpl belongs to the OCD/CRYM superfamily, including the archetype OCD (subfamilies 7 and 11) [2,21], CRYM/ketimine reductase (subfamily 5) [3], AlaDH (subfamily 2) [7,8], L-arginine dehydrogenase (subfamily 10) [22], L-lysine cyclodeaminase (EC 4.3.1.28; subfamily 8) [23], tauroamine and strombine dehydrogenases (EC 1.5.1.23(22); subfamily 3) [24,25], L-2,3-diaminopropionate synthase (subfamily 4) [26], and Pyr2C reductase (from bacteria) (subfamilies 6 and 9) [13] (Fig. 4). TILhpl had a poor relationship to the bacterial Lhpl and mammalian CRYM proteins, in spite of their similar activity, and formed a close but distinct subfamily to many archaeal OCD-like proteins, including AfAlaDH (novel subfamily 1). Surprisingly, two OCD-like proteins from “thermophilic bacteria”, *Thermosediminibacter oceani* (Toce_0467) and *Thermovirga lienii* (Thlie_1581), were closely related to TILhpl rather than (bacterial) Ablhpl and

CpLhpl, suggesting the possibility of horizontal gene transfer between bacteria and archaea.

Putative amino acid sequences of TILhpl contained essential amino acid residues for coenzyme binding (Rossmann-fold motif consisting of Gly-X-Gly-X₂-[Ala/Ser], where X indicates any amino acid) and the catalytic tetrad for interacting (and/or binding) with carboxyl and amino groups of substrate ([Arg/Lys]-Lys-Arg-Asp): Gly¹³⁴-Ala-Gly-Val-Gln-Ala¹³⁹ and Arg³⁹-Lys⁶⁷-Arg¹¹⁰-Asp³⁰³, respectively [2,8] (Fig. 5). Furthermore, TILhpl possessed a specific aspartate residue (Asp¹⁵⁹) for NAD⁺(H)-dependent enzymes of the OCD/CRYM superfamily [2,7,23–26], conforming to the coenzyme specificity, described above.

2.6. Identification of catalytic amino acid residues

It is proposed that three amino acid residues of OCD, E56-D228-K232 (numbering from *P. putida*), are related to the unique cyclization of L-ornithine [2] (Fig. 5). In TILhpl and AfAlaDH, these amino acid residues correspond to L52-V224-A228 and R52-D219-K223, respectively (conserved amino acid residues are underlined). To obtain insight into the catalytic mechanism of OCD/CRYM superfamily enzymes, we constructed three mutants of TILhpl, V224D/A228K (DK mutant), L52E/V224D/A228K (EDK mutant), and L52R/V224D/A228K (RDK mutant). They were overexpressed in *E. coli* cells as a His₆-tagged enzyme and purified with the same procedures as for the wild-type enzyme (Fig. 1F). Approximately 12-fold enhancement of Pyr2C reductase activity (6.7-fold for the oxidation activity for L-proline), but not AlaDH activity, was found in the DK mutant, caused by the increasing k_{cat} value (Tables 1 and 2). On the other hand, when the mutations were combined with L52E and L52R, AlaDH activities for the 2-oxo acids were completely eliminated, whereas Pyr2C reductase activity was the same as in the wild type (Fig. 2C).

2.7. Characterization of TILhplH

Potential T3LHyp dehydratase activity in TILhplH was initially assayed spectrophotometrically in the coupling system with TILhpl (in the presence of NADH). A significant decrease in absorbance at 340 nm was observed as a result of cooperative reactions by TILhplH (T3LHyp → Pyr2C) and TILhpl (Pyr2C → L-proline): 44.6 unit/mg protein of specific activity with T3LHyp. K_m and k_{cat} values for T3LHyp were 0.288 mM and 1710 min⁻¹, respectively, comparable with those of AblhplH (data not shown). On the other hand, optimum temperature for the activity was 80–100 °C, which was significantly higher than that of the (mesophilic) AblhplH (40–45 °C) (Fig. S2B). These results indicated that the TILhplH gene encodes T3LHyp dehydratase with enzymatic properties as a typical (hyper)thermophilic enzyme: this is the first example for archaea.

2.8. Physiological meaning of TILhpl and TILhplH

Although a minimal medium for the cultivation of *T. litoralis* is not available, we found that *T. litoralis* can grow in the complex medium [27] supplemented with L-proline, D-proline or T3LHyp as a sole carbon source, instead of maltose and peptone (data not shown). On the other hand, Pyr2C reductase and T3LHyp dehydratase activities in cell-free extract prepared from *T. litoralis* cells grown on such as carbon source were similar to those on maltose and peptone. These suggested one possibility that similar metabolic pathway of T3LHyp to bacteria and mammalian is operative in *T. litoralis*.

3. Discussion

The discovery of archaeal reductase for Pyr2C revealed that OCD/CRYM superfamily enzymes with this activity are large:

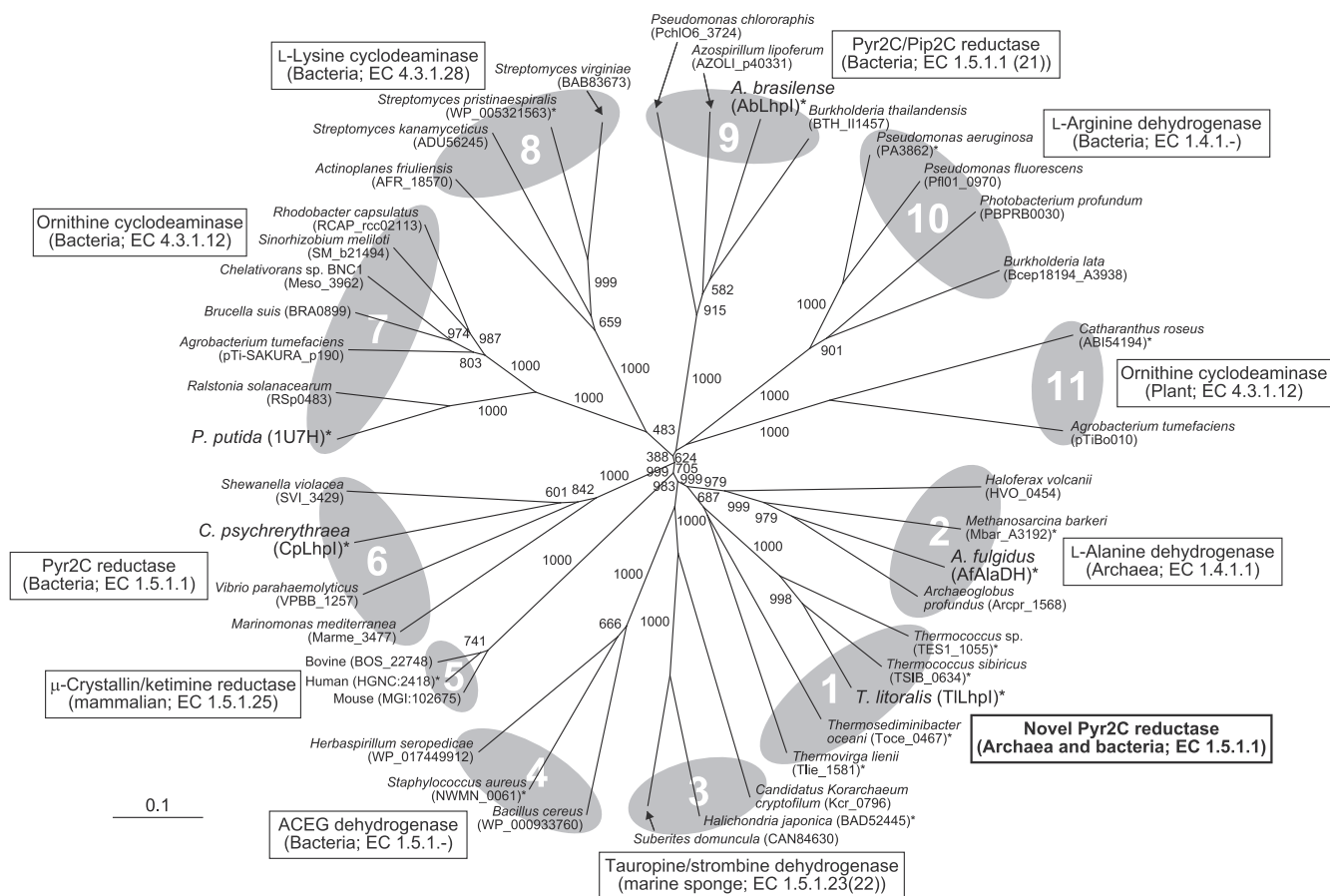


Fig. 4. Phylogenetic tree of OCD/CRYM protein superfamily consisting of eleven subfamilies. The number on each branch indicates the bootstrap value. Proteins with asterisks were used for Fig. 5A.

subfamilies of 1, 5, 6, 7, 9, and 11 at least (Fig. 4). Furthermore, TILhpl (and Ablhpl and Cplhpl) possesses not only Pyr2C reductase activity but also (slight but significantly detectable) AlaDH and NMAlaDH activities. Among OCD/CRYM members, enzymatic reactions by subfamilies 2 and 10 are homologous to AlaDH, and enzymes of subfamilies 3 and 4 catalyze similar reactions to NMAlaDH, in which taurine, glycine, and L-2,3-diaminopropionate are used as the nitrogen donor instead of NH_4^+ , respectively [24–26]. Furthermore, cyclodeaminases for L-ornithine and L-lysine possess the same initial step of the catalytic reaction as AlaDH and NMAlaDH (step 1 in Fig. 1B). This suggests that the origin of L-ProDH (Pyr2C reductase) activity (step 6) is the same as step 1. A common ancestor possessed NAD(P)^+ -dependent dehydrogenation activity toward broad primary and secondary amines, and (strict) substrate specificity convergently evolved in bacteria, mammals, and archaea. If this hypothesis is true, TILhpl acquired catalytic specificity as Pyr2C reductase later than Ablhpl and Cplhpl, because the relative high activity of AlaDH and broad substrate specificity of L-ProDH remain (Fig. 2B and C).

Although it is unclear whether OCD possesses (remaining) oxidative deamination activity for L-amino acid(s) except L-ornithine, the “potential” mechanism to produce Pyr2C (from L-ornithine) by TILhpl corresponds to scheme I, because of the AlaDH activity. Therefore, to obtain evolutionary insight into Pyr2C reductase and OCD, we introduced several specific amino acid residues for OCD in TILhpl by site-directed mutagenesis. Although Asp²²⁸ of OCD (numbering from *P. putida*) plays an important role in all steps of catalysis [2,11], Asp²¹⁹ conserved in AfAlaDH is not involved in catalysis (steps 1 and 2) [8]. Therefore, it may be reasonable that the V244D (and A228K) mutant of TILhpl has no significant effect

on AlaDH activity (Tables 1 and 2, and Fig. 3C), because of the similar mechanism to AfAlaDH, as described above. On the other hand, Glu⁵⁶ of OCD favorably interacts with the δ -amino group of L-ornithine. In CRYM, it is also proposed that Gly⁶⁰ at the equivalent position (numbering from mouse) is important for the binding of a large ligand, T3, because of the small side chain [28]. These insights explain why the substitution of Leu⁵² in hydrophilic glutamate or arginine in TILhpl leads to a complete loss of reductive amination activity for hydrophobic 2-oxo acid substrates (Fig. 3C).

As in our previous proposal [13], dehydratase activity with T3LHyp in the proline racemase superfamily was acquired once at an early evolutionary stage, because TILhpl also forms a single subfamily together with enzymes from bacteria and mammals (Fig. S1). Several (thermophilic) archaea and bacteria possess another proline racemase-like gene instead of the *LhpH* gene within the gene cluster containing the *LhpI* gene (Fig. 1D). The enzymatic function may be interconversion of L- and D-isomer of proline (and/or hydroxyproline), but not dehydration of T3LHyp: Pyr2C is potentially produced from D-proline by FAD-dependent D-ProDH (Fig. 1C). TILhpl (this study; Fig. 2B) and L-ProDH ($\alpha_4\beta_4$) [29] show activities not only for Pyr2C and L-proline but also Δ^1 -piperidine-2-carboxylate and L-pipecolate, respectively, which are involved in the so-called “L-pipecolate pathway” of D-lysine metabolism [16]. Putative L-ProDH genes are also found within the gene cluster. Furthermore, (putative) pyruvate-formate lyase (PFL) and serine/threonine dehydratase genes, producing pyruvate and/or 2-oxobutyrate, are often located within the flanking region of the *LhpI* gene (Fig. 1D). These indicate the possibility that the *TILhpl* gene (and the gene cluster) is also involved not only in T3LHyp but also in D-proline, L-proline and D-lysine metabolism, and several 2-oxo

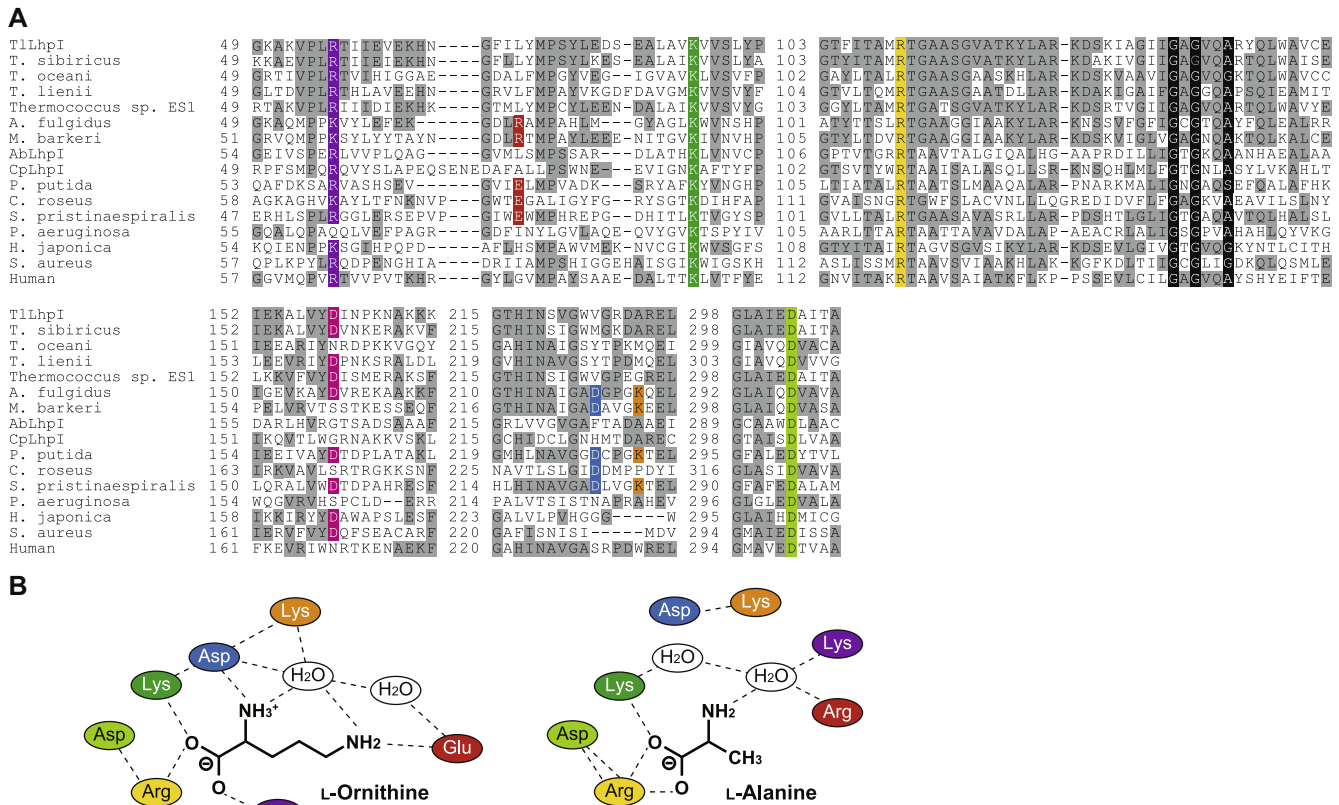


Fig. 5. (A) Partial multiple sequence alignment of deduced amino acid sequences of TlLhpI. Binding sites for a carboxyl group of substrate are shaded in violet, green, yellow and light-green. Aspartate, lysine and glutamate residues, related to the cyclization by OCD, are shaded in blue, orange, and red, respectively. A specific aspartate residue for NAD⁺(H)-dependent enzymes, potentially interacting with 2'- and 3'-hydroxyl groups in the ribosyl moiety of NAD⁺(H), are shaded in pink. Amino acid residues Coenzyme-binding motif of Rossmann-fold are shown as white letters in black boxes. Gray-shaded letters indicate highly conserved amino acid residues. (B) Schematic diagram showing the interactions of L-ornithine (left panel) and L-alanine (right panel), and nearby residues in OCD and AlaDH, respectively. Color of residues correspond to Fig. 5A. (For interpretation of the references to color in this figure legend, the reader is referred to the web version of this article.)

acids. Although *T. litoralis* can grow on T3LHyp as a sole carbon source, Pyr2C reductase (and T3LHyp dehydratase) activity is not significantly induced in cell-free extract, in contrast of bacteria [13], conforming to the putative functions in multiple metabolism described above. Development of gene disruption of *T. litoralis* would be useful for understanding more detailed physiological role(s) of *TlLhpI* gene.

4. Experimental procedures

4.1. General procedures

Basic recombinant DNA techniques were performed as described by Sambrook et al. [30]. PCR was carried out using a GeneAmp PCR System 2700 (Applied Biosystems) for 30 cycles in a 50 µl reaction mixture containing 1 U of KOD FX DNA polymerase (TOYOBO), appropriate primers (15 pmol) and template DNA under the following conditions: denaturation at 98 °C for 10 s, annealing at 50 °C for 30 s and extension at 68 °C for the time periods calculated at an extension rate of 1 kbp min⁻¹. DNA sequencing was carried out using the BigDye Cycle Sequencing Kit ver.3.1 (Applied Biosystems) and appropriate primers with the Genetic Analyzer 3130 (Applied Biosystems). Protein concentrations were determined by the method of Lowry et al. [31] with bovine serum albumin as the standard. SDS-PAGE was performed as described by Laemmli [32].

4.2. Strain and growth conditions

T. litoralis DSM5473 were grown under anaerobic conditions at 80 °C in a complex medium, as described previously [27], in the

absence of sulfur. If necessary, maltose, peptone and yeast extract were omitted, and L-proline, D-proline or T3LHyp (30 mM) was added alternatively.

4.3. Plasmid construction for expression of recombinant proteins

Primer sequences used in this study are shown in Table S1. In this report, the prefixes Tl (*T. litoralis*), Af (*A. fulgidus*), Ab (*A. brasiliense*) and Cp (*C. psychrerythraea*) have been added to gene symbols or protein designations when required for clarity. *TlLhpI* (fusion of OCC_00362 and OCC_00367; see Supplementary Methods) and *TlLhpH* genes (OCC_00387) were amplified by PCR using primers containing appropriate restriction enzyme sites at the 5' and 3' ends and genome DNA of *T. litoralis* as a template. Each amplified DNA fragment was introduced into BamHI-PstI sites in pETDuet-1 (Novagen), a plasmid vector for conferring N-terminal His₆-tag on expressed proteins, to obtain pET/TlLhpI_{WT} and pET/TlLhpH.

4.4. Expression and purification of His₆-tagged recombinant proteins

E. coli BL21(DE3)-RIL (Novagen) harboring the expression plasmid for His₆-tagged proteins was grown at 37 °C to a turbidity of 0.6 at 600 nm in Super broth medium (pH 7.0, 12 g tryptone, 24 g yeast extract, 5 ml glycerol, 3.81 g KH₂PO₄, and 12.5 g K₂HPO₄ per liter) containing 50 mg/liter ampicillin. After the addition of 1 mM isopropyl-β-D-thiogalactopyranoside (IPTG), the culture was further grown for 6 h at 37 °C to induce the expression of His₆-tagged protein. Cells were harvested and resuspended in Buffer A (50 mM sodium phosphate buffer (pH 8.0) containing 300 mM NaCl and 10 mM imidazole). The cells were then

disrupted by sonication for 20 min at appropriate intervals on ice using the Ultra Sonic Disruptor Model UR-200P (TOMY SEIKO Co., Ltd., Tokyo, Japan), and the solution was centrifuged at $108,000\times g$ for 20 min at 4 °C. The supernatant was loaded onto a Ni-NTA Superflow column (Qiagen) equilibrated with Buffer A linked to the BioAssist eZ system (TOSOH). The column was washed with Buffer B (50 mM sodium phosphate buffer (pH 8.0) containing 300 mM NaCl, 10% (v/v) glycerol, and 50 mM imidazole). The enzymes were then eluted with Buffer C (pH 8.0, Buffer B containing 250 mM imidazole instead of 50 mM imidazole), concentrated by ultrafiltration with Centriplus YM-30 (Millipore), dialyzed against 50 mM Tris-HCl buffer (pH 8.0) containing 50% (v/v) glycerol, and stored at -35 °C until use. If necessary, Ablhpl and Cplhpl proteins were prepared, as described previously [13].

The native molecular mass of recombinant proteins was estimated by gel filtration, which was carried out using HPLC with a Multi-Station LC-8020 model II system (TOSOH) at a flow rate of 1 mL min⁻¹. The purified enzyme (~10 mg mL⁻¹) was loaded onto a TSKgel G3000SWXL column (TOSOH) equilibrated with 50 mM Tris-HCl buffer (pH 8.0). A high molecular weight gel filtration calibration kit (GE Healthcare) was used as a molecular marker.

4.5. Enzyme assay

All enzyme assays were performed at 50 °C unless otherwise indicated.

Pyr2C reductase was assayed routinely in the direction of Pyr2C reduction by measuring the oxidization of NADH at 340 nm, using a Shimadzu UV-1800 spectrophotometer (Shimadzu GLC Ltd., Tokyo, Japan). The standard assay mixture contained 10 mM Pyr2C in 50 mM potassium phosphate (pH 6.0) buffer. The reactions were started by the addition of 100 µl of a 1.5 mM NADH solution to a final volume of 1 ml. To assay the reverse reaction, the reaction mixture consisted of 50 mM Bis-tris propane (pH 10.5) and 10 mM L-proline. The reaction was started by the addition of 15 mM NAD⁺ (100 µl) with a final reaction volume of 1 ml. One unit of enzyme activity refers to 1 µmol NADH produced/min. Pyr2C was enzymatically synthesized from T3LHyp, described previously [13].

AlaDH activity was measured as oxidative deamination of L-alanine and as reductive amination of pyruvate. For the oxidative deamination assay, the standard assay mixture contained 50 mM Bis-tris propane (pH 10.5), 10 mM L-alanine, and 1.5 mM NAD⁺. The reductive amination assay mixture consisted of 50 mM Tris-HCl (pH 8.0), 700 mM NH₄Cl, 10 mM pyruvate, and 0.15 mM NADH. For the assay of NMAlaDH activity, 50 mM methylamine was used instead of 700 mM NH₄Cl.

T3LHyp dehydratase was assayed spectrophotometrically in the coupling system with TILhpl. The reaction mixture consisted of 50 mM Tris-HCl (pH 8.0), 0.15 mM NADH, and 10 µg purified TILhpl. The reaction was started by the addition of 100 mM T3LHyp (100 µl) with a final reaction volume of 1 ml. The enzyme was alternatively assayed by the colorimetric method based on the reaction of 2-aminobenzaldehyde with Pyr2C, which yields a yellow reaction product [15]. This method was used to determine the optimum temperature for activity.

4.6. Reaction product analysis

Purified TILhpl (10 µg) was added to the following four mixtures (1 ml): for AlaDH activity, 50 mM Tris-HCl (pH 8.0) buffer containing 10 mM pyruvate (or 2-oxobutyrate), 500 mM NH₄Cl, and 10 mM NADH; for NMAlaDH activity, 50 mM Tris-HCl (pH 8.0) buffer containing 10 mM pyruvate, 100 mM methylamine, and 10 mM NADH; for L-ProDH activity; 50 mM Bis-tris propane (pH 10.5) buffer containing 10 mM L-proline and 10 mM NAD⁺;

for T3LHyp dehydratase activity of TILhpl; 50 mM Tris-HCl (pH 8.0) buffer containing 10 mM T3LHyp, 10 mM NADH, and TILhpl (10 µg). After incubation at 50 °C overnight, each enzyme product was then analyzed by a Hitachi L-8900 amino acid analyzer (Tokyo, Japan), using ion exchange chromatography followed by post-column derivatization with ninhydrin. In the case of L-ProDH activity, the product was further oxidized by the addition of 30% H₂O₂ (20 µl) to the mixture before HPLC analysis [33].

4.7. Zymogram staining analysis

Purified TILhpl was separated at 4 °C on non-denaturing PAGE with 10% (w/v) gel, which was performed by omitting SDS and 2-mercaptoethanol from the solution used in SDS-PAGE. The gels were then soaked in 10 ml staining solution consisting of 50 mM Bis-tris propane (pH 10), 0.25 mM nitroblue tetrazolium (NBT), 0.06 mM phenazine methosulfate (PMS), 10 mM substrate, and 10 mM NAD⁺ at 50 °C for 5 min in the dark. Dehydrogenase activity appeared as a dark blue band.

4.8. Site-directed mutagenesis

The mutation in TILhpl was introduced by sequential steps of PCR [34] using sense and antisense primers (Table S1) and pET/TILhpl_{WT} (for V224D/A228K (DK) mutant) or pET/TILhpl_{DK} (for L52E/V224D/A228K (EDK) and L52R/V224D/A228K (RDK) mutants) as a template. Briefly, the codons used for single mutants were as follows: L52E, CTG → AGG; L52R, CTG → GAG; V224D, GTG → GAC; A228K, GCC → AAG. The coding region of the mutated genes was confirmed by subsequent sequencing in both directions. Mutant proteins were expressed and purified by the same procedures as for the wild-type enzyme.

4.9. Amino acid sequence alignment and phylogenetic analysis

Protein sequences were analyzed using the Protein-BLAST and Clustal W program distributed by DDBJ (DNA Data Bank of Japan) (www.ddbj.nig.ac.jp). Multiple sequence alignment was performed with the following default parameters: Protein Weight Matrix, Gonnet; GAP OPEN, 10; GAP EXTENSION, 0.20; GAP DISTANCES, 5; NO END GAPS, no; ITERATION, none; NUMITER, 1 and CLUSTERING, NJ. The phylogenetic tree was constructed by the neighbor-joining method [35]. Bootstrap resampling was performed 1000 times.

Acknowledgments

This work was partially supported by KAKENHI (25440049) (to S.W.) and HOKTO Research Foundation (to S.W.). We thank Prof. Haruhiko Sakuraba (Faculty of Agriculture, Kagawa University) and Dr. Ryushi Kawakami (Institute of Socio-Arts and Sciences, University of Tokushima) for the gift of *T. litoralis* DSM 5473. Our thanks are extended especially to Dr. Miyuki Kawano-Kawada (Integrated Center for Sciences (INCS), Ehime University) for amino acid analysis.

Appendix A. Supplementary data

Supplementary data associated with this article can be found, in the online version, at <http://dx.doi.org/10.1016/j.fob.2014.07.005>.

References

- [1] Nocek, B., Chang, C., Li, H., Lezondra, L., Holzle, D., Collart, F. and Joachimiak, A. (2005) Crystal structures of Δ^1 -pyrroline-5-carboxylate reductase from human pathogens *Neisseria meningitidis* and *Streptococcus pyogenes*. *J. Mol. Biol.* 354, 91–106.
- [2] Goodman, J.L., Wang, S., Alam, S., Ruzicka, F.J., Frey, P.A. and Wedekind, J.E. (2004) Ornithine cyclodeaminase: structure, mechanism of action, and implications for the mu-crystallin family. *Biochemistry* 43, 13883–13891.

- [3] Hallen, A., Cooper, A.J., Jamie, J.F., Haynes, P.A. and Willows, R.D. (2011) Mammalian forebrain ketimine reductase identified as μ -crystallin; potential regulation by thyroid hormones. *J. Neurochem.* 118, 379–387.
- [4] Cho, K., Fuqua, C., Martin, B.S. and Winans, S.C. (1996) Identification of *Agrobacterium tumefaciens* genes that direct the complete catabolism of octopine. *J. Bacteriol.* 178, 1872–1880.
- [5] Costilow, R.N. and Laycock, L. (1971) Ornithine cyclase (deaminating): purification of a protein that converts ornithine to proline and definition of the optimal assay conditions. *J. Biol. Chem.* 246, 6655–6660.
- [6] Soto, M.J., van Dillewijn, P., Olivares, J. and Toro, N. (1994) Ornithine cyclodeaminase activity in *Rhizobium meliloti*. *FEMS Microbiol. Lett.* 11, 209–214.
- [7] Schröder, I., Vadas, A., Johnson, E., Lim, S. and Monbouquette, H.G. (2004) A novel archaeal alanine dehydrogenase homologous to ornithine cyclodeaminase and μ -crystallin. *J. Bacteriol.* 186, 7680–7689.
- [8] Gallagher, D.T., Monbouquette, H.G., Schröder, I., Robinson, H., Holden, M.J. and Smith, N.N. (2004) Structure of alanine dehydrogenase from *Archaeoglobus*: active site analysis and relation to bacterial cyclodeaminases and mammalian μ -crystallin. *J. Mol. Biol.* 342, 119–130.
- [9] Graupner, M. and White, R.H. (2001) *Methanococcus jannaschii* generates *l*-proline by cyclization of *l*-ornithine. *J. Bacteriol.* 183, 5203–5205.
- [10] Muth, W.L. and Costilow, R.N. (1974) Ornithine cyclase (deaminating). III. Mechanism of the conversion of ornithine to proline. *J. Biol. Chem.* 249, 7463–7467.
- [11] Ion, B.F., Bushnell, E.A., Luna, P.D. and Gauld, J.W. (2012) A molecular dynamics (MD) and quantum mechanics/molecular mechanics (QM/MM) study on ornithine cyclodeaminase (OCD): a tale of two iminiums. *Int. J. Mol. Sci.* 13, 12994–13011.
- [12] Watanabe, S., Morimoto, D., Fukumori, F., Shinomiya, H., Nishiwaki, H., Kawano-Kawada, M., Sasai, Y., Tozawa, Y. and Watanabe, Y. (2012) Identification and characterization of *D*-hydroxyproline dehydrogenase and Δ^1 -pyrroline-4-hydroxy-2-carboxylate deaminase involved in novel *l*-hydroxyproline metabolism of bacteria: metabolic convergent evolution. *J. Biol. Chem.* 287, 32674–32688.
- [13] Watanabe, S., Tanimoto, Y., Yamauchi, S., Tozawa, Y., Sawayama, S. and Watanabe, Y. (2014) Identification and characterization of *trans*-3-hydroxy-*l*-proline dehydratase and Δ^1 -pyrroline-2-carboxylate reductase involved in *trans*-3-hydroxy-*l*-proline metabolism of bacteria. *FEBS Open Bio* 4, 240–250.
- [14] Wu, G., Bazer, F.W., Burghardt, R.C., Johnson, G.A., Kim, S.W., Knabe, D.A., Li, P., Li, X., McKnight, J.R., Satterfield, M.C. and Spencer, T.E. (2011) Proline and hydroxyproline metabolism: implications for animal and human nutrition. *Amino Acids* 40, 1053–1063.
- [15] Visser, W.F., Verhoeven-Duif, N.M. and de Koning, T.J. (2012) Identification of a human *trans*-3-hydroxy-*l*-proline dehydratase, the first characterized member of a novel family of proline racemase-like enzymes. *J. Biol. Chem.* 287, 21654–21662.
- [16] Muramatsu, H., Mihara, H., Kakutani, R., Yasuda, M., Ueda, M., Kurihara, T. and Esaki, N. (2005) The putative malate/lactate dehydrogenase from *Pseudomonas putida* is an NADPH-dependent Δ^1 -piperidine-2-carboxylate/ Δ^1 -pyrroline-2-carboxylate reductase involved in the catabolism of *D*-lysine and *D*-proline. *J. Biol. Chem.* 280, 5329–5335.
- [17] Goytia, M., Chamond, N., Cosson, A., Coatnoan, N., Hermant, D., Berneman, A. and Minoprio, P. (2007) Molecular and structural discrimination of proline racemase and hydroxyproline-2-epimerase from nosocomial and bacterial pathogens. *PLoS One* 2, e885.
- [18] Kawakami, R., Sakuraba, H. and Ohshima, T. (2004) Gene and primary structures of dye-linked *l*-proline dehydrogenase from the hyperthermophilic archaeon *Thermococcus profundus* show the presence of a novel heterotetrameric amino acid dehydrogenase complex. *Extremophiles* 8, 99–108.
- [19] Kawakami, R., Sakuraba, H., Tsuge, H., Goda, S., Katunuma, N. and Ohshima, T. (2005) A second novel dye-linked *l*-proline dehydrogenase complex is present in the hyperthermophilic archaeon *Pyrococcus horikoshii* OT-3. *FEBS J.* 272, 4044–4054.
- [20] Neuner, A., Jannasch, H.W., Belkin, S. and Stetter, K.O. (1990) *Thermococcus litoralis* sp. nov.: a new species of extremely thermophilic marine archaeobacteria. *Arch. Microbiol.* 153, 205–207.
- [21] Trovato, M., Maras, B., Linhares, F. and Costantino, P. (2001) The plant oncogene *rolD* encodes a functional ornithine cyclodeaminase. *Proc. Natl. Acad. Sci. USA* 98, 13449–13453.
- [22] Li, C. and Lu, C.D. (2009) Arginine racemization by coupled catabolic and anabolic dehydrogenases. *Proc. Natl. Acad. Sci. USA* 106, 906–911.
- [23] Gatto Jr, G.J., Boyne 2nd, M.T., Kelleher, N.L. and Walsh, C.T. (2006) Biosynthesis of pipercolic acid by RapL, a lysine cyclodeaminase encoded in the rapamycin gene cluster. *J. Am. Chem. Soc.* 128, 3838–3847.
- [24] Kan-No, N., Matsu-Ura, H., Jikihara, S., Yamamoto, T., Endo, N., Moriyama, S., Nagahisa, E. and Sato, M. (2005) Tauropine dehydrogenase from the marine sponge *Halichondria japonica* is a homolog of ornithine cyclodeaminase/ μ -crystallin. *Comp. Biochem. Physiol.* B141, 331–339.
- [25] Plese, B., Schröder, H.C., Grebenjuk, V.A., Wegener, G., Brandt, D., Natalio, F. and Müller, W.E. (2009) Strombine dehydrogenase in the demosponge *Suberites domuncula*: characterization and kinetic properties of the enzyme crucial for anaerobic metabolism. *Comp. Biochem. Physiol.* B154, 102–107.
- [26] Kobylarz, M.J., Grigg, J.C., Takayama, S.J., Rai, D.K., Heinrichs, D.E. and Murphy, M.E. (2014) Synthesis of *l*-2,3-diaminopropionic acid, a siderophore and antibiotic precursor. *Chem. Biol.* 21, 379–388.
- [27] Sakuraba, H., Kawakami, R., Takahashi, H. and Ohshima, T. (2004) Novel archaeal alanine:glyoxylate aminotransferase from *Thermococcus litoralis*. *J. Bacteriol.* 186, 5513–5518.
- [28] Borel, F., Hachi, I., Palencia, A., Gaillard, M.C. and Ferrer, J.L. (2014) Crystal structure of mouse μ -crystallin complexed with NADPH and the T3 thyroid hormone. *FEBS J.* 281, 1598–1612.
- [29] Monaghan, P.J., Leys, D. and Scrutton, N.S. (2007) Mechanistic aspects and redox properties of hyperthermophilic *l*-proline dehydrogenase from *Pyrococcus furiosus* related to dimethylglycine dehydrogenase/oxidase. *FEBS J.* 274, 2070–2087.
- [30] Sambrook, J., Fritsch, E.F. and Maniatis, T. (2001) *Molecular Cloning: A Laboratory Manual*, 3rd edn, Cold Spring Harbor Laboratory, Cold Spring Harbor, NY.
- [31] Lowry, O.H., Rosebrough, N.J., Farr, A.L. and Randall, R.J. (1951) Protein measurement with the folin phenol reagent. *J. Biol. Chem.* 193, 265–275.
- [32] Laemmli, U.K. (1970) Cleavage of structural proteins during the assembly of the head of bacteriophage T4. *Nature* 227, 680–685.
- [33] Satomura, T., Kawakami, R., Sakuraba, H. and Ohshima, T. (2002) Dye-linked *D*-proline dehydrogenase from hyperthermophilic archaeon *Pyrobaculum islandicum* is a novel FAD-dependent amino acid dehydrogenase. *J. Biol. Chem.* 277, 12861–12867.
- [34] Penning, T.M. and Jez, J.M. (2001) Enzyme redesign. *Chem. Rev.* 101, 3027–3046.
- [35] Saitou, N. and Nei, M. (1987) The neighbor-joining method: a new method for reconstructing phylogenetic trees. *Mol. Biol. Evol.* 4, 406–425.